Decadal Fluctuations in Planetary Wave Forcing Modulate Global Warming in Late Boreal Winter

JUDAH COHEN

Atmospheric and Environmental Research, Inc., Lexington, Massachusetts

MATHEW BARLOW

University of Massachusetts—Lowell, Lowell, Massachusetts

KAZUYUKI SAITO

Frontier Research Center for Global Change, Japan Agency for Marine-Earth Science and Technology, Kanagawa, Japan, and International Arctic Research Center, University of Alaska Fairbanks, Fairbanks, Alaska

(Manuscript received 13 November 2008, in final form 5 March 2009)

ABSTRACT

The warming trend in global surface temperatures over the last 40 yr is clear and consistent with anthropogenic increases in greenhouse gases. Over the last 2 decades, this trend appears to have accelerated. In contrast to this general behavior, however, here it is shown that trends during the boreal cold months in the recent period have developed a marked asymmetry between early winter and late winter for the Northern Hemisphere, with vigorous warming in October–December followed by a reversal to a neutral/cold trend in January–March. This observed asymmetry in the cold half of the boreal year is linked to a two-way stratosphere–troposphere interaction, which is strongest in the Northern Hemisphere during late winter and is related to variability in Eurasian land surface conditions during autumn. This link has been demonstrated for year-to-year variability and used to improve seasonal time-scale winter forecasts; here, this coupling is shown to strongly modulate the warming trend, with implications for decadal-scale temperature projections.

1. Introduction

Global surface temperatures have been in a general warming trend the entire length of the instrumental record, and much of the warming has been attributed to anthropogenic forcings. Though the record extends at least as far back as the midnineteenth century, most of the observed warming has occurred in the most recent 40 yr (Solomon et al. 2007). Deviations from the general upward trend of temperatures exist not only temporally but spatially as well, with the greatest warming anomalies observed over the high-latitude Northern Hemisphere (NH) during the boreal cold season. The skewed warming preferably toward the NH high latitudes during winter—polar and winter amplification—has been attributed to decreasing snow and ice cover (Graversen et al. 2008; Stine et al. 2009).

Observed changes to the climate system have spanned the seasons, including increased snowmelt and early peak river discharge in the spring (Groisman et al. 1994; Rosenzweig et al. 2008), more intense heat waves in the summer (Stott et al. 2004), and a collapse in Arctic sea ice in the fall (Stroeve et al. 2008). Of all the seasons, however, the global climate models (GCMs) predict that winter will experience the greatest warming because of a positive feedback of increased greenhouse gases (GHGs) and a diminished and darker cryosphere (Hansen and Nazarenko 2004). However, news headlines of recent winters (2000/01–present) have been less about the extreme warmth and dwindling cryosphere and more about the severity of winter weather and record snowfalls. Most notably, January 2008 was the coldest for the NH landmasses in the past quarter of a century and the snowiest on record, as measured by satellites, leading global warming skeptics to declare that the earth

Corresponding author address: Judah Cohen, AER, Inc., 131 Hartwell Avenue, Lexington, MA 02421.
E-mail: jcohen@aer.com

DOI: 10.1175/2009JCLI2931.1

has started a protracted cooling trend (e.g., *New York Times*, 2 March 2008). In this note, we analyze the NH cold season temperatures over the past 2 decades. Over this period, global surface temperatures continued to warm at an accelerated rate with the eight warmest years ever recorded occurring after 1998 during the second half of the record being analyzed here. However, our analysis of the observations reveals late-winter damping of upward temperature trends providing asymmetric winter temperature trends in an otherwise secularly warming planet. Furthermore, climate models do not predict the observed temperature trend reversal.

TABLE 1. (left) The Spearman rank correlation of trends and (right) linear trend (°C yr^{-1}) for the 3-month aggregate for OND, JFM, AMJ, and JAS for the surface temperature of extratropical Northern Hemisphere (30°–90°N) landmasses. Those correlations found to be significant using the Student's *t* test at the 90% (95%) confidence limit are listed with a single (double) asterisk and those at the 99% confidence limit are listed in bold.

	OND		JFM		AMJ		JAS	
40-yr trend	**0.68**	0.04	**0.70**	0.05	**0.82**	0.03	**0.77**	0.03
30-yr trend	**0.60**	0.04	**0.48**	0.05	**0.85**	0.04	**0.80**	0.04
20-yr trend	**0.66**	0.06	**0.13**	0.02	**0.73**	0.04	**0.78**	0.04
10-yr trend	0.68**	0.09	−0.09	−0.01	0.56*	0.03	0.42	0.02

2. Data

For model surface temperature data we used the World Climate Research Programme's (WCRP's) Coupled Model Intercomparison Project phase 3 (CMIP3) multimodel dataset (Meehl et al. 2007). For observed surface temperature data we used the Climatic Research Unit (CRU) CRUTEM3 land surface temperature dataset (Brohan et al. 2006). All atmospheric data are taken from the National Centers for Environmental Prediction–National Center for Atmospheric Research (NCEP–NCAR) reanalysis (Kalnay et al. 1996). The October-mean snow cover index merges a satellite-based dataset (Robinson et al. 1993) from 1967 to 2007 and from a historical reconstruction based on in situ observations from 1948 to 1966 (Brown 2000).

3. Results

We tested observed surface temperatures for the extratropical (30°–90°N) NH landmasses for a statistically significant trend for the four seasons: spring [April–June (AMJ)], summer [July–September (JAS)], fall [October–December (OND)], and winter [January–March (JFM)] for the past 40, 30, 20, and 10 yr using CRUTEM3 land surface temperature data (Table 1). We use rank correlation (e.g., Wilks 2006) as a robust measure of the consistency of the trend (the maximum rank correlation of 1.0 would indicate that temperature increases every year), and linear trend as a measure of the trend strength. The deciding factors for dividing the seasons into AMJ, JAS, OND, and JFM are focused on defining winter as JFM. As we will argue below, trends in stratosphere-coupling and snow cover have at least partially contributed to observed surface temperature trends over the period of 1988–2008. Analysis from Cohen et al. (2007) showed that the impact from snow cover forcing in particular and stratosphere–troposphere coupling in general on the phase and magnitude of the Northern annular mode (NAM) is most frequent in January. And, as Baldwin and Dunkerton (2001) have shown, the influence of a stratospheric event on the lower-tropospheric NAM can persist for 2–3 months. Therefore, we felt that any dynamically forced changes from snow cover anomalies or stratosphere–troposphere coupling would be most apparent in the January–March time period.

Three of the seasons show robust warming trends for the most recent 40, 30, and 20 yr, and even at 10 yr the trends are still significant or at least consistent with the longer warming trends. The lone exception is winter where a warming trend is detected at the longer time periods of 40 and 30 yr, but is nearly absent for the last 20 yr and appears to even be slightly negative for the last 10 yr.

The temperature trend for October through December 1988–2007 is shown in Fig. 1a. The trends are mostly consistent with the expectations of a warming planet resulting from increased GHGs; temperatures for the mid- to high latitudes of the Northern Hemisphere have been warming with some regional exceptions. However, the plot of temperature trends for January through March 1989–2008 (Fig. 1b) does not exhibit hemispheric-scale warming; instead, many regions of the mid- to high latitudes have experienced a cooling trend. The pattern of cooling over most of northern Eurasia and the eastern United States, with warming over northeastern Canada, Greenland, and the Middle East, is reminiscent of the negative phase of the NAM. The NAM is the dominant teleconnection pattern of the NH and is characterized by a dipole in the sea level pressure field with one anomaly center over the Arctic and another center of the opposite sign across the midlatitude sector of the North Atlantic and Pacific Oceans (Thompson and Wallace 2000). However, a 2-decade-long cooling trend is not expected based on the known dynamics of global warming. This is especially so, given the decrease in the NH cryosphere prior to the winter season and such a warm beginning to the NH cold half of the year. El Niño–Southern Oscillation (ENSO), the leading mode

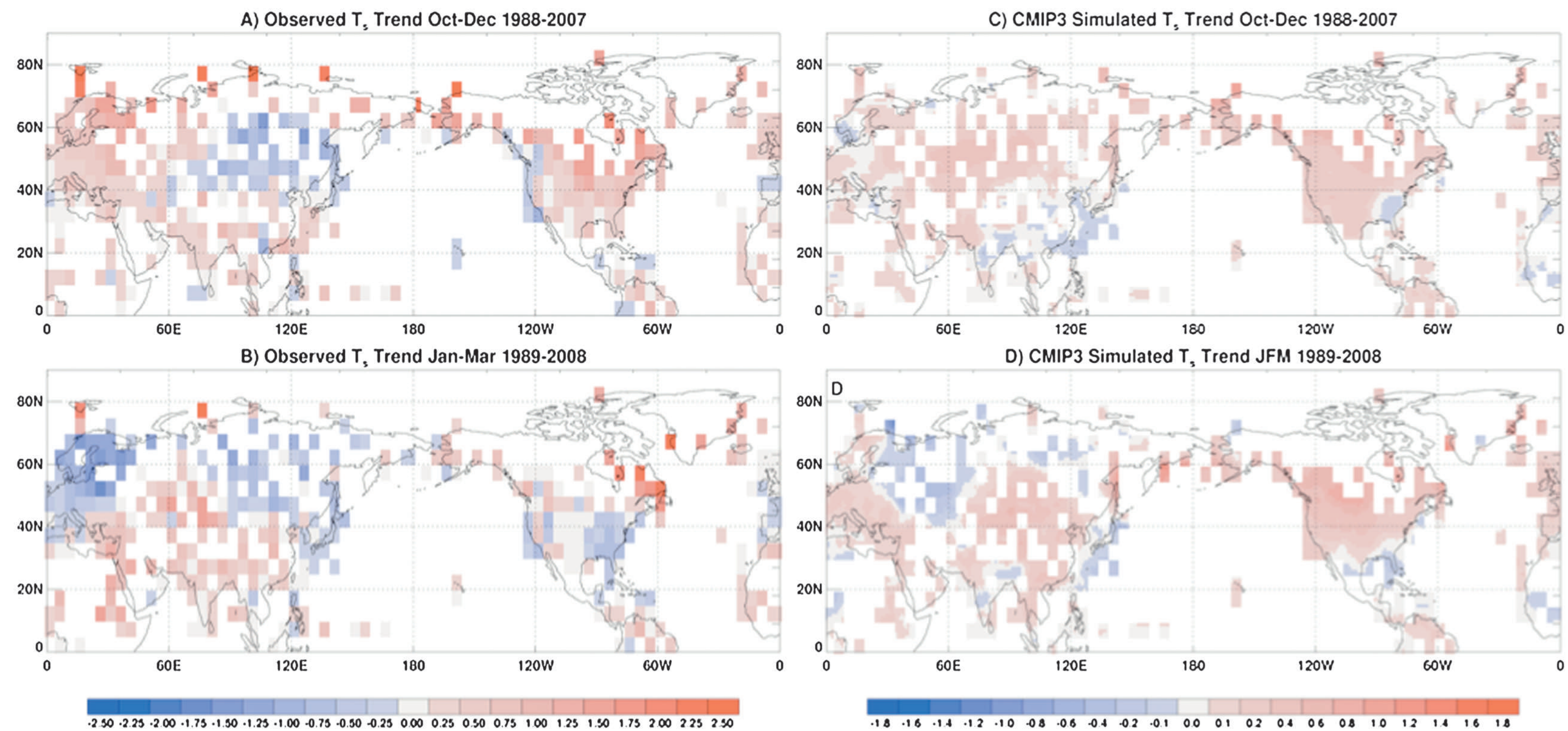

FIG. 1. (a) The decadal trend in October, November, and December land surface temperatures, 1988–2007. (b) The decadal trend in January, February, and March land surface temperatures, 1989–2008. Colored shading (°C); values between −0.25 and 0.25 are shown in gray and missing and ocean values are shown in white. (c) The decadal trend in October, November, and December land surface temperatures, 1988–2007, simulated by CMIP3 GCMs. (d) The decadal trend in January, February, and March land surface temperatures, 1989–2008, simulated by CMIP3 GCMs. Colored shading (°C); values between −0.25 and 0.25 are shown in gray and missing and ocean values are shown in white. Twelve models used for ensemble mean include Bjerknes Center for Climate Research-Bergen Climate Model 2.0 (BCCR-BCM2.0); Canadian Centre for Climate Modelling and Analysis (CCCma) Coupled General Circulation Model, version 3.1 (CGCM3.1); Centre National de Recherches Météorologiques Coupled Global Climate Model, version 3 (CNRM-CM3); Geophysical Fluid Dynamics Laboratory Climate Model version 2.0 (GFDL CM2.0); Goddard Institute for Space Studies (GISS); Institute of Atmospheric Physics (IAP); Istituto Nazionale di Geofisica e Vulcanologia (INGV); Institute of Numerical Mathematics Coupled Model, version 3.0 (INM-CM3.0); L'Institut Pierre-Simon Laplace Coupled Model, version 4 (IPSL CM4); Meteorological Institute of the University of Bonn ECHO-G Model (MIUBECHOG); Max Planck Institute Ocean Model (MPI-OM); and Hadley Centre Global Environmental Model version 1–Met Office (HadGEM1–UKMO). Please refer to Meehl et al. (2007) for more details on the individual models.

of interannual global climate variability, also cannot be evoked as influential in the observed 2-decade temperature trends. The period began and ended with strong La Niña events with a strong El Niño in the middle. Furthermore, we regressed the Niño-3.4 index with surface temperatures and computed the observed trends both with and without the temperature anomalies associated with ENSO variability and found ENSO to have little impact on recent temperature trends (not shown).

Do GCMs forced with increasing GHGs simulate the temperature trends for the period of 1988–2008 similar to the observed trends? As discussed in the introduction, GCM modeling studies predict future warming for all four boreal seasons with winter amplification and with preferential warming over the continents relative to the oceans. Also in Fig. 1, we plot the mean simulated temperature trend from an ensemble of models used in the CMIP3 project for both OND (Fig. 1c) and JFM (Fig. 1d) of 1988–2008. Model-simulated trends show widespread hemispheric warming for both seasons. Thus, the atmosphere–ocean coupled models forced with increased GHGs are correctly simulating the OND hemispheric warming trend, but not the observed JFM cooling trend over many parts of the NH extratropical landmasses.

What can explain mid- to late-winter NH tropospheric cooling of a magnitude that negates increasing GHGs, decreasing ozone, a diminished cryosphere, and a warm start in the troposphere during the NH cold months? While natural variability is to be expected even under a secular global warming trend, it is difficult to explain asymmetric temporal trends in the cool half of the boreal year based on known modes of variability.

We propose anomalies and trends in stratosphere–troposphere coupling as a significant forcing of the observed winter temperature trends. Planetary-scale waves that propagate from the troposphere into the stratosphere control the zonal-mean stratospheric circulation and its variability (Charney and Drazin 1961; Matsuno 1970). More recent work suggests that the zonal-mean stratospheric circulation can in turn exert a downward influence on the zonal-mean tropospheric circulation (Baldwin and Dunkerton 2001).

Stratospheric temperatures are predicted to cool in response to tropospheric warming forced by anthropogenic climate change (Pawson et al. 1998). How the cooling is distributed may not be solely dependent on radiative changes, but also dynamical ones. The cooling is predicted to be greatest in the polar stratosphere because of more frequent positive polarity events of the NAM and the Southern annular mode (SAM) forced by increased GHGs and decreased stratospheric ozone (Shindell et al. 1999; Thompson and Solomon 2002; Gillett and Thompson 2003). Positive trends in the NAM and SAM would result in polar stratospheric cooling and tropical stratospheric warming; and while mean hemispheric stratospheric temperatures have been observed to cool, the cooling is most robust in the tropics while temperature trends in the extratropics are not statistically significant (Thompson and Solomon 2005). Therefore, not only have winter tropospheric temperatures unexpectedly cooled, polar stratospheric temperatures have unexpectedly warmed (Cohen and Barlow 2005; see also Fig. 2d). Furthermore, polar stratospheric cooling has been observed in the Southern Hemisphere but not in the Northern Hemisphere; so, what is forcing the asymmetry between the Northern and Southern polar stratospheres?

It has been demonstrated that tropospheric circulation anomalies associated with the NAM originate in the stratosphere and propagate down to the surface (Baldwin and Dunkerton 2001). In an effort to better understand the origins and timing of stratosphere–troposphere coupling, an index was developed and is referred to as the stratosphere–troposphere coupling index (STCI). This index demonstrates a preference for stratosphere–troposphere coupling in the December–January time frame (Cohen et al. 2007). This suggests that upwelling energy generated by tropospheric Rossby waves in the fall is most likely to influence the polarity of the stratospheric NAM index in January, which leads to a same-sign polarity of the tropospheric NAM index in January and the subsequent winter months. It was further demonstrated that this midwinter stratosphere–troposphere coupling is linked to the previous Eurasian October snow cover.

The STCI and October snow cover area index from 1948/49 through 2007/08 are plotted in Fig. 2a. Here we extend this land–atmosphere coupling from interannual- to decadal-scale variability and trends. The last 20 yr of both time series are characterized by a *statistically* significant increasing trend. This increasing trend in stratosphere coupling and snow cover extent forces more frequent negative polarity of the NAM and its associated temperature pattern. As will be shown below, this pattern is associated with a clear *decrease* in temperatures during late boreal winter over the same time period, a decrease that is made all the more remarkable by the secular global warming occurring throughout the rest of the year. The trend in October NH snow cover shows an overall increasing frequency over a large and coherent region of Eurasia (Fig. 2b). An increase in October Eurasian snow cover has been shown to force upwelling tropospheric energy associated with Rossby waves into the stratosphere in subsequent months, but in particular in December (Saito et al. 2001; Gong et al.

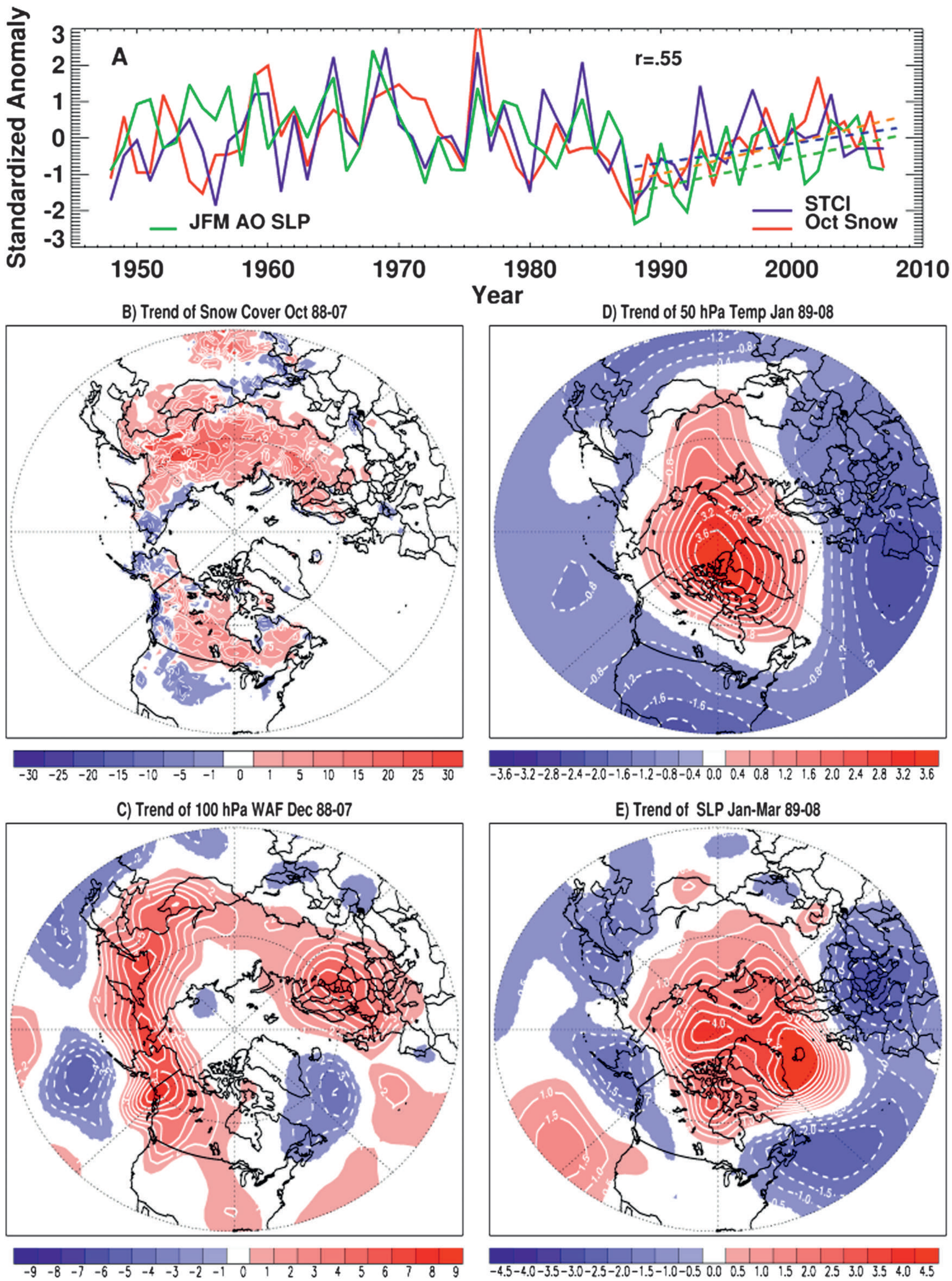

FIG. 2. (a) Plot of the normalized anomalies for the stratosphere–troposphere coupling index (blue), October Eurasian snow cover (red) for the years 1948/49 through 2007/08, and the JFM NAM index (green; multiplied by −1 for ease of comparison) 1949–2008. Also plotted is the linear trend for the most recent 20 yr (solid line). (b) Decadal trend in frequency of October snow cover in percent, 1988–2007. (c) Decadal trend in December upward component of 100-hPa wave activity flux ($m^2\ s^{-2}$) ($\times 5 \times 10^1$), 1988–2007. (d) Decadal trend in January 50-hPa temperatures (°C), 1989–2008. (e) Decadal trend in January, February, and March sea level pressure (hPa), 1989–2008. (b)–(e) Positive trend values (red) and negative trend values (blue) are denoted.

2003; Cohen et al. 2007; Fletcher et al. 2009). Dynamical arguments for the link between snow cover and vertically propagating energy from Rossby waves are beyond the scope of this paper (please refer to these references and further references cited within for full dynamical arguments). Trends of this upwelling energy, referred to as upward wave activity flux (WAF), reveal a 2-decade-long increasing trend over the region of increasing snow cover and in the region of greatest variability of the hemispheric WAF (Fig. 2c). Such a trend has been shown to increase stratosphere–troposphere coupling resulting in more frequent stratospheric warmings. Consistent with the increasing trend, there has been an unprecedented increase in the frequency of the 20-yr period of 1988–2008, with no observed major midwinter warmings (MMW) in the first half of the record and at least nine observed MMW in the latter half of the record (Manney et al. 2005; Charlton and Polvani 2007).

The increased upwelling energy from the troposphere into the stratosphere in December would most directly impact stratospheric temperatures in January; polar stratospheric temperature trends over the past 20 yr exhibit warming (Fig. 2d) despite the opposite forcing from increased GHGs, depleted ozone, and predictions of polar stratospheric cooling. Stratospheric circulation anomalies then propagate down through the troposphere all the way to the surface and can force one polarity of the NAM index predominately for up to 3 months (Baldwin and Dunkerton 2001). Trends in SLP for the months of January–March (Fig. 2e) show a dipole of increasing pressure over the high latitudes and decreasing pressures over the midlatitudes, especially in the North Atlantic sector. This pattern of variability closely resembles the negative polarity of the NAM pattern of variability. In Fig. 2a we also included the JFM NAM index, (multiplied by -1 for ease of comparison) and not surprisingly the NAM index is observed to be in a statistically significant decreasing trend over the 20-yr period since 1989. The negative NAM trend in the late-winter months is also consistent with the observed polar stratospheric warming in January for the same period (Baldwin and Dunkerton 2001; Cohen et al. 2007). Therefore, the increased snow cover in October, the increased WAF in the late fall, and the changes in the stratospheric circulation in midwinter force a lower-tropospheric response that closely resembles the negative polarity of the NAM index beginning in January and continuing through the late-winter months. Presumably, once the dynamically forced cooling has come to its natural conclusion in the late winter and early spring, radiative forced warming resumes.

Finally, in Fig. 3a, we plot the trend of JFM NH temperatures, but first we remove the temperature anomalies regressed with the NAM index over the period. The temperature trend is qualitatively changed from one of mixed temperature trends or even one of cooling to one of clearly warming. We plot in Fig. 3b the difference between Fig. 3a and Fig. 1b, which gives the decadal temperature trend for JFM attributable to NAM variability during the 20-yr period. The negative trend in the NAM index over the past 2 decades has contributed much of the observed cooling over the period. In Fig. 3c we repeat the analysis in Fig. 3b, but the temperature anomalies regressed with the areal extent of October Eurasian snow cover are removed prior to computing the difference from Fig. 1b. The result is qualitatively the same as in Fig. 3b; a large percentage of the decadal temperature trend for JFM is attributable to the increasing snow cover trend during the 20-yr period. We computed the area-weighted pattern correlation for the extratropical NH between Figs. 3b and 3c, and the value is equal to 0.83. The biggest difference between the two plots is the magnitude, with the degree of cooling associated with the snow cover equal to about 40% of the cooling associated with the NAM. This value is consistent with the correlation of $\sim$0.6 computed between Eurasian snow cover and the STCI.

We argue that the positive trend in snow cover has contributed a significant fraction of the observed cooling in eastern North America and northern Eurasia, where snow cover is significantly correlated with winter temperatures (Cohen and Fletcher 2007). Repetition of the analysis in Fig. 3c with the STCI instead provides essentially the same result (not shown). Therefore, much of the recently observed late-winter cooling across the NH is a response to increased October Siberian snow cover, increased WAF mainly over Eurasia, and increased stratosphere–troposphere coupling forcing a dynamical response in the hemispheric circulation. This dynamical forcing has resulted in both stratospheric polar warming and lower-tropospheric cooling over the NH landmasses and has largely masked the global warming trend that is much more apparent earlier in the spring, summer, and fall. While the bulk of the cooling is linearly associated with this mechanism, there appear to be secondary factors as well, which we are investigating.

Coupled GCMs have been shown to poorly simulate stratosphere–troposphere coupling and its associated link with snow cover extent. Hardiman et al. (2008) demonstrated that while the correlation between observed October snow cover extent and the STCI is close to 0.6, in the coupled GCMs that participated in CMIP3, the correlations for all GCMs are clustered around zero. Furthermore, the correlation between December WAF and January SLP is also much lower in the CMIP3 GCMs than that observed. These deficiencies in coupled

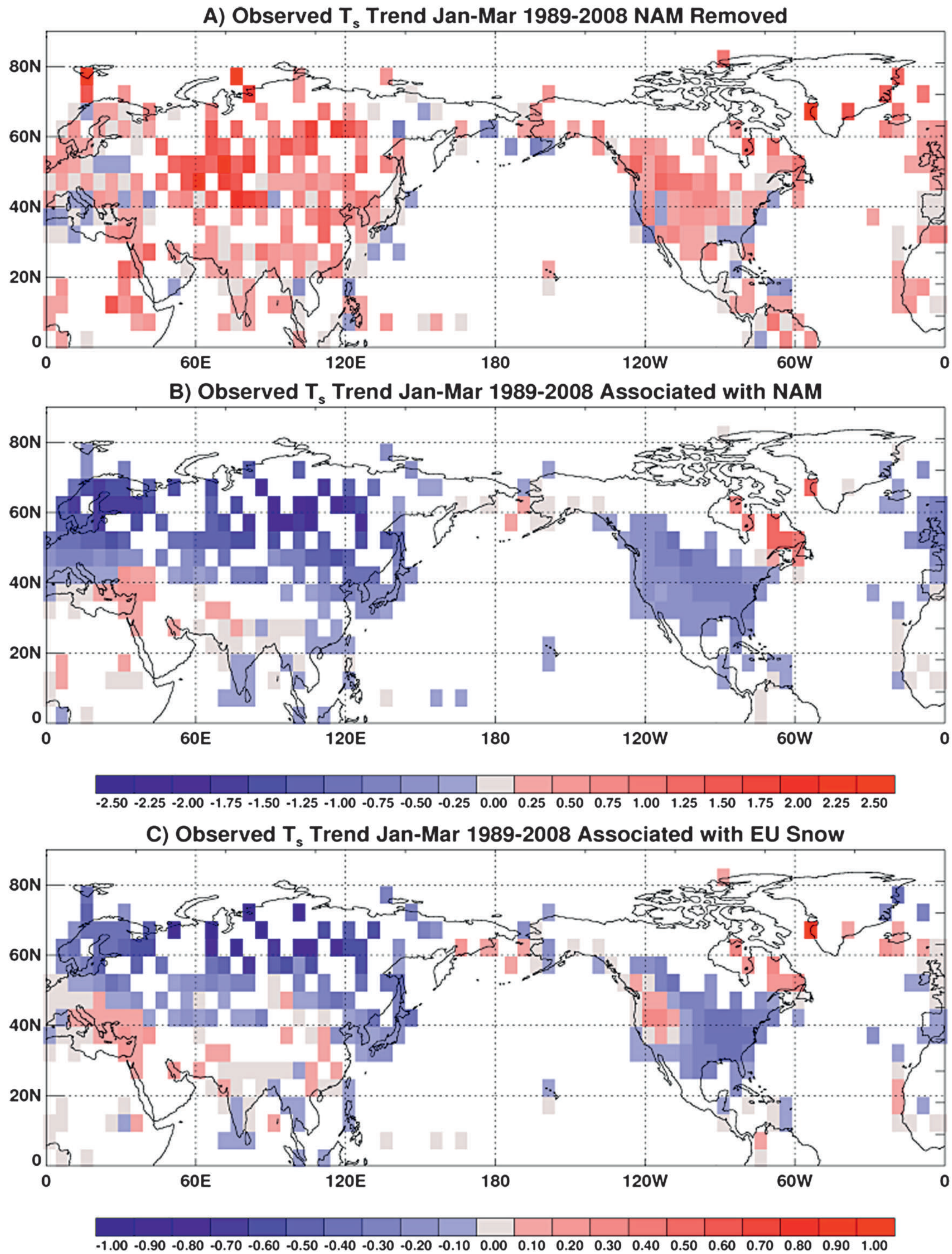

FIG. 3. (a) The decadal trend in January, February, and March land surface temperatures, 1989–2008, after the regressed values of temperature with the concomitant NAM have been removed. (b) The difference between (a) and Fig. 1b. (a),(b) Colored shading (°C); values between −0.25 and 0.25 are shown in gray and missing and ocean values are shown in white. (c) The difference between the decadal trend in January, February, and March land surface temperatures, 1989–2008, after the regressed values of temperature with the prior October Eurasian snow cover extent have been removed, and Fig. 1b. (c) Colored shading (°C); values between −0.1 and 0.1 are shown in gray and missing and ocean values are shown in white.

GCMs would make it highly unlikely for GCMs to simulate observed temperature trends resulting from trends in snow cover and/or stratosphere–troposphere coupling.

4. Conclusions

Over the past 4 decades the globe has experienced accelerated warming, with the majority of that warming occurring in the most recent 2 decades. When the NH cold months are analyzed in aggregate, the observed trends are consistent with expectations: there is almost universal warming, with the largest warming trend biased toward higher latitudes. However, when the early and late months of the cold season are analyzed separately, the two periods are observed to have notable asymmetric temperature trends. For large regions of the extratropical Northern Hemisphere landmasses, the warming is skewed toward the first half of the cold season. A marked trend reversal appears in January, with hemispheric-wide warming in OND but large areas of cooling in JFM and concomitant polar stratospheric warming.

Whether or not this trend reversal continues, it is important to understand the physics of the underlying mechanism for a more complete understanding and more accurate predictions for anthropogenically forced climate change; the trend reversal also provides a useful model test.

What dynamic forcings could contribute to reversing the radiative warming forced by both increased GHGs and decreased planetary albedo resultant of a shrinking cryosphere? Our analysis argues that the temperature trend reversal commences in the stratosphere where increased absorption of anomalous vertical wave activity flux reverses the polar cooling trend to a warming trend, which preferentially occurs in January. The descent of the circulation anomalies from the stratosphere to the troposphere initiates a trend reversal in lower-tropospheric temperatures in the months of January–March. The surface temperature trend pattern is most closely associated with the negative polarity of the NAM, which has been linked with leading stratospheric circulation anomalies. These circulation anomalies are, in turn, linked with increasing Eurasian snow cover in the fall, consistent with changes to the near-surface forcing of vertical wave activity by diabatic cooling (Ringler and Cook 1999). An observed increasing trend in Eurasian snow cover is the most likely boundary condition for partially forcing hemispheric trends over the past 2 decades that has heretofore been identified.

It is expected that global warming will not necessarily be uniform but may have large variations at regional scales as the circulation dynamics adjust to the changing radiative forcing and cryospheric conditions. Here we have identified a clear asymmetry in recent boreal winter trends and shown that circulation changes link the recent late-winter surface cooling trend and polar stratospheric warming trend to changes in fall snow cover and subsequent stratosphere–troposphere coupling. This argues for a dynamic cause to the observed late-winter changes that are opposed to the long-term tropospheric warming trends and stratospheric cooling trends forced partially or in full by radiative effects of increased GHGs, decreased ozone, and a shrinking cryosphere.

Acknowledgments. We thank P. Kushner for his suggestion of removing the NAM from the temperature trends. JC is supported by the National Science Foundation Grant ATM-0443512 and MB was supported by National Science Foundation Grants ATM-0621737, ATM-0603555, and EAR-0811099, and NOAA Grant NA080AR4310592. KS is supported by the National Science Foundation under Cooperative Agreement ARC-0327664. We acknowledge the modeling groups, the Program for Climate Model Diagnosis and Intercomparison (PCMDI) and the WCRP's Working Group on Coupled Modelling (WGCM) for their roles in making the WCRP CMIP3 multimodel dataset available. Support of this dataset is provided by the Office of Science, U.S. Department of Energy.

REFERENCES

Baldwin, M. P., and T. J. Dunkerton, 2001: Stratospheric harbingers of anomalous weather regimes. *Science,* **294,** 581–584.

Brohan, P., J. J. Kennedy, I. Harris, S. F. B. Tett, and P. D. Jones, 2006: Uncertainty estimates in regional and global observed temperature changes: A new dataset from 1850. *J. Geophys. Res.,* **111,** D12106, doi:10.1029/2005JD006548.

Brown, R. D., 2000: Northern Hemisphere snow cover variability and change 1915–97. *J. Climate,* **13,** 2339–2355.

Charlton, A. J., and L. M. Polvani, 2007: A new look at stratospheric sudden warmings. Part I: Climatology and modeling benchmarks. *J. Climate,* **20,** 449–469.

Charney, J. G., and P. G. Drazin, 1961: Propagation of planetary-scale disturbances from the lower into the upper atmosphere. *J. Geophys. Res.,* **66,** 83–109.

Cohen, J., and M. Barlow, 2005: The NAO, the AO, and global warming: How closely related? *J. Climate,* **18,** 4498–4513.

——, and C. Fletcher, 2007: Improved skill for Northern Hemisphere winter surface temperature predictions based on land–atmosphere fall anomalies. *J. Climate,* **20,** 4118–4132.

——, M. Barlow, P. J. Kushner, and K. Saito, 2007: Stratosphere–troposphere coupling and links with Eurasian land surface variability. *J. Climate,* **20,** 5335–5343.

Fletcher, C., S. C. Hardiman, P. J. Kushner, and J. Cohen, 2009: The dynamical response to snow cover perturbations in a large ensemble of atmospheric GCM integrations. *J. Climate,* **22,** 1209–1222.

Gillett, N. P., and D. W. J. Thompson, 2003: Simulation of recent Southern Hemisphere climate change. *Science,* **302,** 273–275.

Gong, G., D. Entekhabi, and J. Cohen, 2003: Modeled Northern Hemisphere winter climate response to realistic Siberian snow anomalies. *J. Climate,* **16,** 3917–3931.

Graversen, R. G., T. Mauritsen, M. Tjernstrom, E. Kallen, and G. Svensson, 2008: Vertical structure of recent Arctic warming. *Nature,* **541,** 53–56.

Groisman, P. Ya., T. R. Karl, and R. W. Knight, 1994: Observed impact of snow cover on the heat valance and the rise of continental spring temperatures. *Science,* **263,** 198–200.

Hansen, J., and L. Nazarenko, 2004: Soot climate forcing via snow and ice albedos. *Proc. Natl. Acad. Sci. USA,* **101,** 423–428.

Hardiman, S. C., P. J. Kushner, and J. Cohen, 2008: Investigating the ability of general circulation models to capture the effects of Eurasian snow cover on winter climate. *J. Geophys. Res.,* **113,** D21123, doi:10.1029/2008JD010623.

Kalnay, E., and Coauthors, 1996: The NCEP/NCAR 40-Year Reanalysis Project. *Bull. Amer. Meteor. Soc.,* **77,** 437–471.

Manney, G. L., K. Kruger, J. L. Sabutis, S. A. Sena, and S. Pawson, 2005: The remarkable 2003–2004 winter and other recent warm winters in the Arctic stratosphere since the late 1990s. *J. Geophys. Res.,* **110,** D04107, doi:10.1029/2004JD05637.

Matsuno, T., 1970: Vertical propagation of stationary planetary waves in the winter Northern Hemisphere. *J. Atmos. Sci.,* **27,** 871–883.

Meehl, G. A., C. Covey, T. Delworth, M. Latif, B. McAvaney, J. F. B. Mitchell, R. J. Stouffer, and K. E. Taylor, 2007: The WCRP CMIP3 multimodel dataset: A new era in climate change research. *Bull. Amer. Meteor. Soc.,* **88,** 1383–1394.

Pawson, S., K. Labitzke, and S. Leder, 1998: Stepwise changes in stratosphere temperature. *Geophys. Res. Lett.,* **25,** 2157–2160.

Ringler, T. D., and K. H. Cook, 1999: Understanding the seasonality of orographically forced stationary waves: Interactions between mechanical and thermal forcing. *J. Atmos. Sci.,* **56,** 1154–1174.

Robinson, D. A., F. Dewey, and R. Heim Jr., 1993: Northern Hemispheric snow cover: An update. *Bull. Amer. Meteor. Soc.,* **74,** 1689.

Rosenzweig, C., and Coauthors, 2008: Attributing physical and biological impacts to anthropogenic climate change. *Nature,* **453,** 353–357.

Saito, K., J. Cohen, and D. Entekhabi, 2001: Evolution in atmospheric response to early-season Eurasian snow cover anomalies. *Mon. Wea. Rev.,* **129,** 2746–2760.

Shindell, D. T., R. L. Miller, G. A. Schmidt, and L. Pandolfo, 1999: Simulation of recent northern winter climate trends by greenhouse-gas forcing. *Nature,* **399,** 452–455.

Solomon, S., D. Qin, M. Manning, M. Marquis, K. Averyt, M. M. B. Tignor, H. L. Miller, and C. Zhenlin, Eds., 2007: *Climate Change 2007: The Physical Science Basis*. Cambridge University Press, 996 pp.

Stine, A. R., P. Huybers, and I. Y. Fung, 2009: Changes in the phase of the annual cycle of surface temperature. *Nature,* **457,** 435–440.

Stott, P. A., D. A. Stone, and M. R. Allen, 2004: Human contribution to the European heatwave of 2003. *Nature,* **432,** 610–614.

Stroeve, J., M. Serreze, S. Drobot, S. Gearhead, M. Holland, J. Maslanik, W. Meir, and T. Scambos, 2008: Arctic sea ice extent plummets in 2007. *Eos, Tans. Amer. Geophys. Union,* **89**, doi:10.1029/2008EO020001.

Thompson, D. W. J., and J. M. Wallace, 2000: Annular modes in the extratropical circulation. Part I: Month-to-month variability. *J. Climate,* **13,** 1000–1016.

——, and S. Solomon, 2002: Interpretation of recent Southern Hemisphere climate change. *Science,* **296,** 895–899.

——, and ——, 2005: Recent stratospheric climate trends as evidenced in radiosonde data: Global structure and tropospheric linkages. *J. Climate,* **18,** 4785–4795.

Wilks, D. S., 2006: *Statistical Methods in the Atmospheric Sciences*. 2nd ed. Academic Press, 467 pp.